A NUMERICAL METHOD TO REMOVE THE HYDRODYNAMIC INSTABILITY GENERATED IN TIME-DOMAIN SIMULATIONS OF ACOUSTIC PROPAGATION IN A LINED FLOW DUCT

Yuanyuan Deng, Antoni Alomar, Didier Dragna, Marie-Annick Galland
Univ Lyon, Ecole Centrale de Lyon, INSA Lyon Université Claude Bernard Lyon I, CNRS,
Laboratoire de Mécanique des Fluides et d'Acoustique, UMR 5509, France

ABSTRACT

A partial gradient term suppression (GTS) method aiming at removing hydrodynamic instabilities generated during acoustic propagation along a lined flow duct is presented. Time-domain simulations are conducted to assess impacts of the partial GTS method based on the NASA Grazing Incidence Tube (GIT) benchmark experiment. The effectiveness of the partial GTS method for removing hydrodynamic instabilities is shown. However the sound pressure is underestimated by several dBs for certain frequencies especially in the low Helmholtz number range. It is found that a relatively accurate prediction of acoustic propagation can be obtained with partially suppressing the mean flow gradient term, in particular for high Helmholtz number.

1. INTRODUCTION

Time-domain approach is well chosen for dealing with broadband problems. However when acoustic waves propagate along the lined duct with mean flow, the arising instability issues lead to the inaccurate predictions of the acoustic field. Since the instability has been revealed through many experiments, a considerable amount of research has been conducted to the study of hydrodynamic instabilities. Various numerical techniques to remove or at least attenuate instabilities related with liners have been proposed. The strategies to remove instabilities can be classified into three classes, which are using coarse meshes and selective filtering [1, 2], taking account of viscous effects [3, 4] and substituting the LEE by related and stable equations [5–9]

This paper presents that the partial GTS method, originally proposed for avoiding the generation of instabilities in shear flows, is also valid for suppressing hydrodynamic instabilities generated during the acoustic propagation in a lined flow duct. The paper is organized as follows. The configuration of the model, the governing equations and the numerical schemes are presented in Section 2. The partial GTS method is presented in Section. 3. Finally, in Section 4, impacts of the partial GTS method on the hydrodynamic instabilities and acoustic propagation are finally discussed.

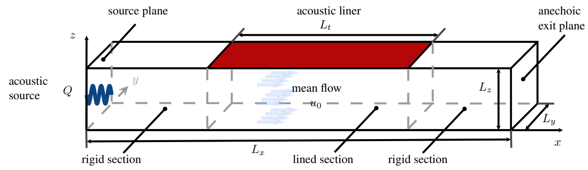

Figure 1. Schematic view of NASA Grazing Incidence Tube (GIT)

2. NUMERICAL MODEL

2.1 Set-up of the NASA experiments

The set-up configuration in the paper is based on the NASA GIT test [10], which has been already considered in many papers. The duct consists of 3 sections with dimensions of $L_x \times L_y \times L_z$ ($L_x = 0.812$ m, $L_y = L_z = 0.0508$ m). The liner is located in the middle of the upper wall with a length $L_t = 0.406$ mm as shown in Fig. 1.

The liner used is a ceramic tubular liner, referred to as CT57. The pressure is measured by 31 microphones placed along the lower wall. The source is harmonic, with frequencies from 500 Hz to 3000 Hz, in steps of 100 Hz. It is located at the input section of the duct. Experiments are conducted for 5 flow speeds, with average Mach numbers M equal to 0, 0.079, 0.172, 0.255, 0.335 and 0.4. At the duct exit, although the exit impedance is measured by NASA, it will be further assumed that the termination is anechoic. The speed of sound in air c_0 is 344.283 m/s. The density of air ρ_0 is 1.29 $\mathrm{kg/m^3}$.

2.2 Governing equations

Acoustic propagation in the duct is governed by the linearized Euler equations (LEE). Assuming the mean flow is homentropic and neglecting the gradient of mean pressure, the LEE can be expressed as:

$$\frac{\partial p}{\partial t} + u_0 \frac{\partial p}{\partial x} + \rho_0 c_0^2 \frac{\partial u}{\partial x} + \rho_0 c_0^2 \frac{\partial v}{\partial z} = Q \tag{1a}$$

$$\frac{\partial u}{\partial t} + u_0 \frac{\partial u}{\partial x} + v \frac{\mathrm{d}u_0}{\mathrm{d}z} + \frac{1}{\rho_0} \frac{\partial p}{\partial x} = 0 \tag{1b}$$

$$\frac{\partial v}{\partial t} + u_0 \frac{\partial v}{\partial x} + \frac{1}{\rho_0} \frac{\partial p}{\partial z} = 0 \tag{1c}$$

where p, u and v are the acoustic pressure and components of the acoustic velocity along the x and z-direction, respectively.

The mean flow velocity profile is given by:

$$u_0\left(z\right) = M\frac{n_t+1}{n_t}\left(1-\left|1-2z\right|^{n_t}\right), \qquad (2)$$

where M is the Mach number corresponding to the mean velocity. The parameter n_t specifies the flow profile and can be related to the boundary layer thickness. The displacement thickness, defined by:

$$\delta = \int_0^{1/2}\left(1-\frac{u_0(z)}{u_0(1/2)}\right)\mathrm{d}z, \qquad (3)$$

is equal to $\delta = 1/[2(n_t+1)]$.

2.3 Time-domain solver

The LEE are solved using high order finite-difference time-domain methods. For the interior gird points, the optimized fourth-order finite-difference schemes of Bogey & Bailly [11] are adopted for the calculating the spatial derivative and the selective filters of Bogey *et al.* [12] are used for filtering the grid-to grid oscillations. For the boundary points, the non-centered finite-difference schemes of Berland *et al.* [13] are employed together with these selective filters of Berland *et al.* [13]. The optimized fourth order six-stage Runge-Kutta algorithm of Berland *et al.* [14] is employed for time integration. To avoid computing the convolution integral, the admittance time-domain boundary condition proposed in Troian *et al.* [15] is used. The admittance of the liner is obtained by a fit of the educed values provided by Jones *et al.* [10] for $M = 0.335$. In this case, two pairs of complex-conjugate poles are sufficient to have a good match from 500 Hz up to 3 kHz.

The source term Q in Eq. (1a) is chosen as

$$Q\left(x,z,t\right) = \lambda(t)\exp\left(-\frac{x^2+\left(z-L_z/2\right)^2}{B_s^2}\ln 2\right). \qquad (4)$$

The Gaussian half-width of the source B_s is set to 5.3×10^{-3} m. An impulsive source is centered at $x_s = 5\times10^{-2}$ m. $\lambda(t)$ is defined as:

$$\lambda(t) = \frac{t-t_s}{t_c}\exp\left(-\frac{\left(t-t_s\right)^2}{t_c^2}\ln 2\right)H(t) \qquad (5)$$

where $t_s = 8\times10^{-4}$ s and $t_c = 1.4\times10^{-4}$ s respectively stand for a time shift and a parameter determining the frequency content of the source signal and $H(t)$ is the unit step function.

The time step is 2×10^{-6} s and the whole simulation lasts for 2×10^{-2} s. The grid is uniform along the x-direction with a mesh spacing $\Delta x = 1.1\times10^{-3}$ m. In both sides of the duct, damping zones are implemented to ensure no reflection by the ends of the duct. In these zones, the mesh spacing is gradually increased with a stretching factor of 3 %. Along the z-direction, the mesh size is $\Delta z = \Delta x$ in the middle of the duct, and it decreases gradually towards walls with a shrinking factor of 1%.

3. GRADIENT TERM SUPPRESSION TECHNIQUES

A natural generalization of the original GTS method is used here to suppress the instability, consisting of a partial suppression of the gradient term instead of a complete suppression. Eq. (1b) is modified by adding a coefficient ϵ in front of the term of $\mathrm{d}u_0/\mathrm{d}z$. Consequently, Eq. (1b) turns to

$$\frac{\partial u}{\partial t} + u_0\frac{\partial u}{\partial x} + \epsilon\frac{\mathrm{d}u_0}{\mathrm{d}z}v + \frac{1}{\rho_0}\frac{\partial p}{\partial x} = 0, \qquad (6)$$

where ϵ adjusts the strength of the mean flow gradient term and ranges from 1 to 0.

Combining Eqs. (1a), (6) and (1c) leads to the wave equation:

$$\frac{\mathrm{D}}{\mathrm{D}t}\left(\frac{1}{c_0^2}\frac{\mathrm{D}^2 p}{\mathrm{D}t^2} - \nabla^2 p\right) + (\epsilon+1)\frac{\mathrm{d}u_0}{\mathrm{d}z}\frac{\partial^2 p}{\partial x\partial z} = \frac{\mathrm{D}^2 Q}{\mathrm{D}t^2} \quad (7)$$

where $\mathrm{D}/\mathrm{D}t = \partial/\partial t + u_0\,\partial/\partial x$ is the material derivative. In particular, the Lilley's equation is recovered for $\epsilon = 1$. The decrease of ϵ from 1 to 0 is thus equivalent to transforming the original Lilley's equation, which sustains unstable modes, to a simplified form of Lilley's equation which appears to be inherently stable [5]. In addition, decreasing ϵ from 1 to 0 diminishes the refraction term proportional to $\mathrm{d}u_0/\mathrm{d}z$ in the original Lilley's equation by a factor of two. A gradual suppression of the instability is then expected when diminishing the value of ϵ. It should be noted that the effect of the partial GTS method on acoustic propagation is mostly observed at low frequencies [5]. It is because that with the decrease of ϵ, the coefficient in front of the refraction term $\frac{\mathrm{d}u_0}{\mathrm{d}z}\frac{\partial^2 p}{\partial x\partial z}$ in Eq. (7) turns to $1+\epsilon$ while the coefficient is 2 in the original Lilly's equation. As a result, the influence of ϵ on acoustic propagation is comparatively weak in the high frequency range.

4. RESULTS

The time series of the pressure obtained at a virtual microphone located on the rigid wall at $x = 0.5\,L$ are shown in Fig. 2 for several values of ϵ. The successive appearance of the initial acoustic pulse and the instability is observed. The impact of ϵ is mainly on the instability component: decreasing ϵ induces a delay in the emergence of the instability. For $\epsilon = 0.3$ and 0 no instability appears within the simulation time.

The resulting SPL and phase of the acoustic pressure along the duct wall opposite to the liner are also studied at different frequencies and for different values of ϵ. To assess the effectiveness of the GTS, another quantity of interest, namely the insertion loss (IL), is also compared with the experimental results.

The NASA GIT benchmark deals with small Helmholtz numbers (a non-dimensional frequency $\omega \leq 2.8$). To examine the performance of the partial GTS method for high Helmholtz numbers, simulations are conducted for a duct whose height $H = 0.508$ m is 10 times larger than the one

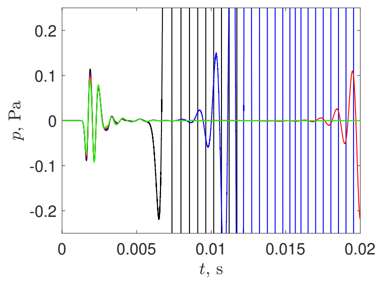

Figure 2. Time series of pressure on the rigid wall at $x = 0.5\,L$ for: black $\epsilon = 1$, blue $\epsilon = 0.7$, red $\epsilon = 0.5$, brown $\epsilon = 0.3$ and green $\epsilon = 0$.

of the NASA GIT duct. These results have been obtained already and will be presented in the presentation.

5. CONCLUSION

An analysis of the partial GTS method for suppressing hydrodynamic instabilities in a lined flow duct has been performed. The effectiveness of this method has been shown for removing the instabilities in time-domain simulations based on the NASA GIT benchmark. The SPL was however underestimated by several dBs for certain frequencies. In particular, a total suppression of the mean flow gradient term seems too severe to accurately predict sound propagation in a lined flow duct, while a partial suppression of this term seems to provide an acceptable prediction, especially in the high frequency range.

Since the effectiveness of the partial GTS method has been proved, other techniques proposed for dealing with shear instabilities [6–9, 16] can also be considered

6. ACKNOWLEDGMENTS

Y. Deng is sponsored by China Scholarship Council as a Ph.D. student in Ecole Centrale de Lyon. This work was performed within the framework of the Labex CeLyA of the Université de Lyon, within the programme "Investissements d'Avenir"(ANR-10-LABX-0060/ANR-16-IDEX-0005) operated by the French National Research Agency (ANR). The authors would like to thank Dr. Michael Jones (NASA) for providing the data for the NASA GIT benchmark.

7. REFERENCES

[1] C. Richter and F. Thiele, "Stability of time explicit impedance models," in *13th AIAA/CEAS Aeroacoustics Conference*, AIAA Paper 2007-3538, (Rome, Italy), American Institute of Aeronautics and Astronautics, 2007.

[2] E. Brambley and G. Gabard, "Time-domain implementation of an impedance boundary condition with boundary layer correction," *Journal of Computational Physics*, vol. 321, pp. 755–775, Sept. 2016.

[3] D. Marx and Y. Aurégan, "Effect of turbulent eddy viscosity on the unstable surface mode above an acoustic liner," *Journal of Sound and Vibration*, vol. 332, pp. 3803–3820, July 2013.

[4] D. Khamis and E. J. Brambley, "Viscous effects on the acoustics and stability of a shear layer over an impedance wall," *J. Fluid Mech.*, vol. 810, pp. 489–534, 2017.

[5] C. Bogey, C. Bailly, and D. Juvé, "Computation of flow noise using source terms in linearized euler's equations," *AIAA journal*, vol. 40, no. 2, pp. 235–243, 2002.

[6] R. Ewert and W. Schr "Acoustic perturbation equations based on flow decomposition via source filtering," *Journal of Computational Physics*, vol. 188, no. 2, pp. 365 – 398, 2003.

[7] J.-H. Seo and Y. J. Moon, "Perturbed compressible equations for aeroacoustic noise prediction at low mach numbers," *AIAA journal*, vol. 43, no. 8, pp. 1716–1724, 2005.

[8] X. Zhang, X. Chen, and J. Gill, "Gradient term filtering for stable sound propagation with linearized euler equations," in *20th AIAA/CEAS Aeroacoustics Conference*, 06 2014.

[9] Y. Sun, R. Fattah, S. Zhong, and X. Zhang, "Stable time-domain caa simulations with linearised governing equations," *Computers and Fluids*, vol. 167, pp. 187 – 195, 2018.

[10] M. Jones, W. Watson, and T. Parrott, "Benchmark data for evaluation of aeroacoustic propagation codes with grazing flow," in *11th AIAA/CEAS Aeroacoustics Conference, AIAA Paper 2005-2853*, pp. 1–18, 2005.

[11] C. Bogey and C. Bailly, "A family of low dispersive and low dissipative explicit schemes for flow and noise computations," *Journal of Computational Physics*, vol. 194, pp. 194–214, Feb. 2004.

[12] C. Bogey, N. de Cacqueray, and C. Bailly, "A shock-capturing methodology based on adaptative spatial filtering for high-order non-linear computations," *Journal of Computational Physics*, vol. 228, no. 5, pp. 1447–1465, 2009.

[13] J. Berland, C. Bogey, O. Marsden, and C. Bailly, "High-order, low dispersive and low dissipative explicit schemes for multiple-scale and boundary problems," *Journal of Computational Physics*, vol. 224, pp. 637–662, June 2007.

[14] J. Berland, C. Bogey, and C. Bailly, "Low-dissipation and low-dispersion fourth-order Runge–Kutta algorithm," *Computers & Fluids*, vol. 35, pp. 1459–1463, Dec. 2006.

[15] R. Troian, D. Dragna, C. Bailly, and M.-A. Galland, "Broadband liner impedance eduction for multimodal acoustic propagation in the presence of a mean flow," *Journal of Sound and Vibration*, vol. 392, pp. 200–216, 2017.

[16] J. H. Seo and Y. J. Moon, "Linearized perturbed compressible equations for low mach number aeroacoustics," *Journal of Computational Physics*, vol. 218, no. 2, pp. 702–719, 2006.